Auxin signaling and vascular cambium formation enables storage metabolism in cassava tuberous roots

David Rüscher[1], José María Corral García[1], Anna Vittoria Carluccio[2,4], Patrick A.W. Klemens[3], Andreas Gisel[2,5], Livia Stavolone[2,4], Ekkehard Neuhaus[3], Frank Ludewig[1**], Uwe Sonnewald[1], Wolfgang Zierer[1*]

* To whom correspondence should be addressed. Tel.: +49 9131 85 25238

** Present address: KWS Saat SE, Grimsehlstraße 31, 37574 Einbeck, Germany

[1] Friedrich-Alexander-University Erlangen-Nuremberg, Department of Biology, Division of Biochemistry, Staudtstrasse 5, 91058 Erlangen, Germany

[2] International Institute for Tropical Agriculture, Oyo Road, Ibadan 200001, Oyo State, Nigeria

[3] Technical University Kaiserslautern, Department of Biology, Division of Plant Physiology, Erwin-Schrödinger-Str. 22, 67663 Kaiserslautern

[4] Institute for Sustainable Plant Protection, CNR, Bari, Italy

[5] Institute for Biomedical Technologies, CNR, Bari, Italy

Author contact: David Rüscher: david.ruescher@fau.de, José María Corral García: jose.m.corral@fau.de, Anna Vittoria Carluccio: annavittoria.carluccio@ipsp.cnr.it, Patrick A.W. Klemens: pklemens@rhrk.uni-kl.de, Andreas Gisel: A.Gisel@cgiar.org, Livia Stavolone: l.stavolone@cgiar.org, Ekkehard Neuhaus: neuhaus@rhrk.uni-kl.de, Frank Ludewig: frank.ludewig@kws.com, Uwe Sonnewald: uwe.sonnewald@fau.de, Wolfgang Zierer: wolfgang.zierer@fau.de

Highlight

Auxin-mediated activation of secondary growth and subsequent *KNOX/BEL* expression coincides with active storage metabolism in xylem parenchyma cells of the cassava tuberous root.

Abstract

Cassava storage roots are among the most important root crops worldwide and represent one of the most consumed staple foods in Sub-Saharan Africa. The vegetatively propagated tropical shrub can form many starchy tuberous roots from its stem. These storage roots are formed through the activation of secondary root growth processes. However, the underlying genetic regulation of storage root development is largely unknown. Here we report on distinct structural and transcriptional changes occurring during the early phases of storage root development.

A pronounced increase in auxin-related transcripts and the transcriptional activation of secondary growth factors, as well as a decrease in gibberellin-related transcripts was observed during the early stages of secondary root growth. This was accompanied by increased cell wall biosynthesis, increased most notably during the initial xylem expansion within the root vasculature. Starch storage metabolism was activated only after the formation of the vascular cambium. The formation of non-lignified xylem parenchyma cells and the activation of starch storage metabolism coincided with increased expression of the *KNOX/BEL* genes *KNAT1*, *PENNYWISE* and *POUND-FOOLISH*, indicating their importance for proper xylem parenchyma function.

Keywords

Auxin, Cassava, Development, Gibberellin, Parenchyma, Root, Starch, Storage, Transcriptomics, Xylem

Abbreviations

AGAMOUS-LIKE (*AGL*), *ADP-GLUCOSE PYROPHOSPHORYLASE* (*AGPase*), *AMYLASE* (*AMY*), *AINTEGUMENTA* (*ANT*), *APETALA 1* (*AP1*), *A. thaliana* (*Arabidopsis thaliana*), *AUXIN RESPONSE FACTOR* (*ARF*), *AUXIN RESISTANT 1* (*AUX1*), *AUXIN RESISTANT/INDOLE-3-ACETIC ACID INDUCIBLE* (*AUX/IAA*), *UDP-APIOSE/UDP-XYLOSE SYNTHASE* (*AXS*), *STARCH BRANCHING ENZYME* (*BE*), *BLADE-ON-PETIOLE* (*BOP*), Co (cortex), *CLAVATA3/ESR-RELATED* (*CLE*), *CELLULOSE SYNTHASE-LIKE D* (*CSLD*), *CELL WALL INVERTASE* (*cwINV*), *CYCLIN D3;1* (*CycD3;1*), developing storage roots (DSR), Ed (endodermis), *FRUCTOSE KINASE* (*FRK*), FWER (family-wise error rate), *GIBBERELLIN-2-OXIDASE* (*GA2OX*), *GIBBERELLIN-3-OXIDASE* (*GA3OX*), *GIBBERELLIN-20-OXIDASE* (*GA20OX*), *UDP-GLUCURONIC ACID EPIMERASE* (*GAE*), *GALACTOSE KINASE* (*GalK*), *GRANULE-BOUND STARCH SYNTHASE* (*GBSS*), *GDP-FUCOSE SYNTHASE* (*GER*), *GRETCHEN HAGEN 3/INDOLE-3-ACETIC ACID-AMIDO SYNTHASE* (*GH3*), *GIBBERELLIN INSENSITIVE DWARF 1* (*GID1*), *GDP-MANNOSE PYROPHOSPHORYLASE* (*GMP*), *CLASS III HOMEODOMAIN LEUCINE ZIPPER TRANSCRIPTION FACTORS* (*HD-ZIP III*), *HEXOKINASE* (*HXK*), *KNOTTED-LIKE FROM ARABIDOPSIS THALIANA 1* (*KNAT1*), *ENT-KAUREN SYNTHASE* (*KS*), *LOB DOMAIN-CONTAINING PROTEIN* (*LBD*), log2FC (log2 fold-change), non-bulked root (NBR), P (phloem), Pc (procambium), PCA (principal component analysis), Pd (periderm), *PHABULOSA* (*PHB*), *PHOSPHOGLUCOMUTASE* (*PGM*), *STARCH PHOSPHORYLASE* (*PHS*), *PHOSPHOGLUCOSE ISOMERASE* (*PGI*), *PHOSPHOMANNOSE ISOMERASE* (*PMI*), *PHOSPHOMANNOSE MUTASE* (*PMM*), *POUND-FOOLISH* (*PNF*), *PENNYWISE* (*PNY*), PP (primary phloem), *PETAL LOSS* (*PTL*), PX (primary xylem), *PHLOEM INTERCALATED WITH XYLEM* (*PXY*), Rd (rhizodermis), *SMALL AUXIN UPREGULATED RNA* (*SAUR*), *STARCH SYNTHASE* (*SS*), *SUCROSE SYNTHASE* (*SUS*), *TREHALOSE-6-PHOSPHATE SYNTHASE/PHOSPHATASE* (*TPS/TPP*), *UDP-GLUCOSE DEHYDROGENASE* (*UGDH*), *UDP-GLUCOSE PYROPHOSPHORYLASE* (*UGPase*), *UDP-XYLOSE EPIMERASE* (*UXE*), *UDP-XYLOSE SYNTHASE* (*UXS*), *VACUOLAR INVERTASE* (*vINV*), VC (vascular cambium), VR (vascular ray), *WUSCHEL-RELATED HOMEOBOX* (*WOX*), X (xylem), XP (xylem parenchyma), XV (xylem vessel).

Introduction

Cassava (*Manihot esculenta*) is an agronomically important root crop species grown in tropical and subtropical regions of the world (Carvalho *et al.*, 2018). Over 60% of the global annual cassava yield is produced in Sub-Saharan Africa (http://faostat3.fao.org/), despite the crop being almost exclusively grown by smallholder farmers with limited resources. While grown on a large total field area, the yield per hectare is often low due to suboptimal agronomic practice, missing fertilizer and/or high pathogen incidence. In addition, the cassava breeding progress lags behind other crops like maize, wheat or rice. Current cassava breeding focuses mostly on resistance and complex yield traits, e.g. dry matter content and root yield. A better understanding of cassava storage root development could facilitate breeding or biotechnological efforts aimed at improved storage root yield.

Cassava is clonally propagated through the planting of stem cuttings from which new shoots and roots can emerge. Cassava storage roots develop from stem-derived roots through the formation of a vascular cambium and subsequent secondary root growth (Chaweewan and Taylor, 2015; Mehdi et al., 2019). The molecular mechanisms of secondary growth have mainly been studied in the model systems *Arabidopsis thaliana* and poplar (*Populus trichocarpa*) and while many details are still elusive much has been learned in the recent past (Fischer *et al.*, 2019). The vascular cambium develops from a procambium in between primary phloem and xylem tissue and controls the formation of secondary phloem and xylem (Ragni and Greb, 2018; Fischer *et al.*, 2019). The initiation and maintenance of meristematic stem cells is largely regulated by the phytohormone auxin (Snow, 1935; Björklund *et al.*, 2007; Agusti *et al.*, 2011). Auxin is synthesized in the shoot apex and moves into the root via a polar transport mechanism governed by auxin influx (AUX) and efflux carriers (PIN) (Bennett *et al.*, 1996; Carraro *et al.*, 2012; Robert *et al.*, 2015). Here it leads to the formation of a stem cell organizer via CLASS III HOMEODOMAIN LEUCINE ZIPPER (HD-ZIPIII) transcription factor activity that regulates the position and maintenance of the vascular cambium (Smetana *et al.*, 2019). Auxin is not the only phytohormone involved in vascular cambium development. Cytokinin and gibberellin have a complex interplay with auxin in the meristem of poplar stems (Immanen *et al.*, 2016). Cytokinin plays a major role in defining cell identities and controlling cell division, while GA promotes cell elongation and the deposition of secondary cell walls and lignification (Eriksson *et al.*, 2000; Biemelt *et al.*, 2004; Fischer *et al.*, 2019).

While some studies have recently indicated the importance of early auxin signaling events, as well as reduced gibberellin signaling during storage root formation in sweet potato (Noh *et al.*, 2010; Firon *et al.*, 2013; Singh *et al.*, 2019), less is known about storage root initiation in cassava. The importance of auxin and gibberellin, as well as other phytohormones could be shown for *in vitro* root formation (Sojikul *et al.*, 2015; Utsumi *et al.*, 2020). In addition, Ding *et al.* (2020) recently analyzed the impact of transcriptional and post-transcriptional regulation of starch and cell wall metabolism as well as hormone response genes in already established cassava storage roots. However, processes during the early stages of storage root development remain to be elucidated in cassava.

In this study, we focused on the morphological and transcriptional changes occurring during the early stages of storage root development under field and controlled greenhouse conditions. The transition of stem-derived roots towards starch storing tuberous roots was analyzed via RNA sequencing and qRT-PCR, as well as detailed histological studies. We identified pronounced auxin

signaling events and the activation of secondary growth factors, as well as decreased gibberellin signaling in the transition stages. This was accompanied by extensive regulation of cell wall biosynthesis genes, which likely is the result of the initial xylem expansion occurring during secondary growth within the root vasculature. After establishment of a vascular cambium, increased amounts of non-lignified parenchyma cells were observed. Starch storage was initiated in parenchyma cells and the corresponding samples displayed the transcriptional profiles of a starch storage crop. Interestingly, the activation of starch storage metabolism coincided with increased expression of the *KNOX/BEL* genes *KNAT1*, *PENNYWISE* and *POUND-FOOLISH*, indicating their importance for proper xylem parenchyma function. Our study provides insight into the formation of the cassava vascular cambium and secondary growth and provides a framework for subsequent genetic studies.

Material and Methods

Planting material and growth conditions

Cassava stem sticks of genotype TME419 were planted in a field at IITA Ibadan, Nigeria towards the end of the rainy season. Root samples were taken from three individual sticks and frozen in liquid nitrogen at 30 dap, 38 dap and 60 dap. The samples were used for transcriptome analysis. Cassava stem sticks of genotype TME7 were grown in a green house in Erlangen, Germany under a light regime of 12 h light and 12 h dark. Temperature was kept at a constant of 30°C and 60% relative humidity. Two nodal-derived root samples from the basal end of the stick were taken from four sticks each at 22, 26, 30, 34, 38, 42 and 60 dap. Approximately 5 mm root pieces of the primary bulking area at the proximal end of the root were stored in 70% EtOH for subsequent microscopy. Root tips were cut off and the root was frozen in liquid nitrogen. These samples were used for qRT-PCR.

Determination of soluble sugars, starch and free amino acids

Soluble sugars, starch and amino acids were measured as described previously (Obata *et al.*, 2020).

Histology and microscopy

Histology and microscopy was performed as described previously (Mehdi et al., 2019).

RNA extraction, RNA sequencing and qRT-PCR

Total RNA was extracted from TME419 roots by combining a modified CTAB-based extraction method (Li *et al.*, 2008) with subsequent spin-column purification. Approximately 500mg of sample material was grinded in liquid nitrogen and mixed with pre-heated 1 mL CTAB extraction buffer (2% CTAB, 2% PVP-40, 20 mM Tris–HCl, pH 8.0, 1.4 M NaCl, 20 mM EDTA). Samples were incubated at 65ºC for 15 min and centrifuged at 15000 rpm at 4ºC for 5 min. The supernatant was transferred and mixed with an equal volume of cold chloroform: isoamyl alcohol (24:1) before centrifugation at 15000 rpm for 10 min. The supernatant was mixed with 0.6 volume of cold isopropanol and centrifuged at maximum speed for 20 min. The pellet was washed with 70% ethanol, air-dried and dissolved in nuclease free- water. After DNaseI treatment, the resulting RNA was cleaned up using the kit RNA clean & concentrator™ (Zymo Research, USA) according to manufacturer's instructions.

RNA samples were depleted of ribosomal RNA (Ribo-Zero rRNA Removal Kit Plant, Illumina) and sequenced with Illumina technology to obtain an average of 20 million paired-end reads. Raw files containing between 21 million and 60 million paired-end reads.

RNA extraction of TME7 roots was performed using the Spectrum Plant Total RNA Kit (Sigma-Aldrich, St. Luis, MO, USA). cDNA was generated from 0.5 µg RNA using the RevertAid H Minus Reverse Transcriptase as indicated by the manufacturer (Thermo Fisher Scientific, Waltham, MA, USA). The cDNA was 1:10 diluted and quantification of gene expression was examined using GoTaq® qPCR Master Mix (Promega, Madison, USA). The assay was mixed in a 96-well plate and measured in an AriaMx Real-time PCR System (Agilent, Santa Clara, USA). The results were analyzed using the $2^{-\Delta\Delta Ct}$ method (Livak and Schmittgen, 2001).

Read trimming and mapping

FastQ files containing the raw sequencing reads were quality checked using FastQC (v. 0.11.5; http://www.bioinformatics.babraham.ac.uk/projects/fastqc/) and MultiQC (v. 1.8; https://multiqc.info/). Adapter and quality trimming was performed in two steps utilizing the k-mer trimming tool BBduk (v. 38.96; https://sourceforge.net/projects/bbmap/) with its provided adapter sequences. A k-mer length of 21 was set allowing a minimum k-mer length of 11 and two mismatches. Reads < 35 nucleotides or an average quality < 20 were excised, as well as individual bases below a quality of 20 at the ends of the read. The resulting FastQ files were mapped to the *M. esculenta* genome (v.7.1; https://genome.jgi.doe.gov/portal/pages/dynamicOrganismDownload.jsf?organism=Mesculenta) in two passes using STAR (v.2.5.0a; Dobin *et al.* (2012); https://github.com/alexdobin/STAR). The resulting BAM files were indexed and deduplicated employing samtools (v.1.7; Li *et al.* (2009) ; http://www.htslib.org/). Read counting was performed using the program featureCounts (v.1.5.0; Liao *et al.* (2013); http://bioinf.wehi.edu.au/featureCounts/). Only primary reads were counted. Trimmed, mapped and deduplicated read counts are available in table S1 at Dryad digital repository (https://doi.org/10.5061/dryad.0cfxpnw0t). All aforementioned programs were used under Linux (Ubuntu v. 18.04 LTS).

Data analyses

Log2 fold-change (log2FC) and its standard error were estimated in R (v. 3.6.2) utilizing the Bioconductor package DESeq2 (https://bioconductor.org/packages/release/bioc/html/DESeq2.html; Love *et al.* (2014)) on individual pairs. Wald's test was used to calculate p-values between pairs, which were adjusted after Bonferroni's family wise error rate (FWER). Genes with $|\log2FC| \geq 1$ and FWER ≤ 0.05 were accepted as differentially expressed genes (DEGs). Enrichment analysis were conducted with a one-sided Fisher's exact test using the Bioconductor package clusterProfiler. (https://bioconductor.org/packages/release/bioc/html/clusterProfiler.html; Yu *et al.* (2012)). Enrichments with FWER ≤ 0.05 were accepted as significant. Kyoto Encyclopedia of Genes and Genomes (KEGG) orthology (KO) terms, cassava and tale cress identifiers were taken from an annotation file published with the genome. Pathway and regulatory networks were constructed through publication- and database mining (STRING [https://string-db.org/], BioGRID [https://thebiogrid.org/] and TAIR [https://www.arabidopsis.org/]). In the text, cassava genes were described by their best *A. thaliana* hit based on BLASTP similarity.

Results and discussion

Phenotypic and metabolic characterization of cassava root growth in the field

Stem sticks of cassava genotype TME419 were planted in a field in Ibadan, Nigeria for up to 60-days to evaluate cassava storage root growth. The plants were carefully dug up and sampled at 30 days after planting (dap), 38 dap and 60 dap. Two types of roots were observed during the experiment, one of which progressed towards storage roots. These root types were subsequently called non-bulked roots (NBR) and developing storage roots (DSR). While the two root types were difficult to distinguish at 30 dap, they became distinct due to increased stiffness and darkening around 38 dap (Fig. 1A). This color change is likely the result of root periderm formation, a protective tissue layer that contains an enrichment of phenolic compounds (Campilho *et al.*, 2020). The periderm is formed during secondary growth making this root color change indicative for this process. Plants analyzed at 60 dap had clearly distintuishable tuberous roots that had already bulked considerably (Fig. 1A). Potential and visually distinguishable, developing storage roots were analyzed for their soluble sugars, starch, proteins and amino acids on a dry matter basis (Fig. 1B).

Soluble sugar concentrations increased linear over time with sucrose showing the highest abundance in comparison to glucose and fructose, indicating increased sucrose delivery and cleavage in storage roots. While there is a slight increase in starch concentration between 30 and 38 dap, an exponentially higher accumulation is observed between 38 and 60 dap. This is accompanied by a profound increase in free total amino acid concentrations. However, no elevation in protein concentration was observed. The high amino acid level at 60 dap was mainly due to accumulation of nitrogen-rich amino acids glutamine, glutamate, aspartate and especially arginine indicating increased delivery of nitrogen compounds from source tissues into storage roots (Fig. 1C). In contrast to many other root and tuber crops, cassava does not produce high abundant storage proteins (Vanderschuren *et al.*, 2014), which could explain the high levels of free nitrogen-rich amino acids.

Together, the phenotypic and metabolic data suggested the onset of secondary root growth between timepoint 30 and 38 dap, and the onset of storage metabolism in the tuberous root between timepoints 38 and 60 dap.

Transcriptome analysis on cassava root types

To learn more about the underlying gene regulation of storage root formation, RNA-seq was performed on the different root samples. All replicates of each condition clustered together in a principal component anlysis (PCA) on log transformed counts, demonstrating that no obvious sample outliers are present in the data set (Fig. 2A). The different timepoints and tissues separated along PC1 and PC2, respectively with PC1 accounting for 64% and PC2 for 20% of variance. This indicated a higher influence of time than tissue on the cassava root transcriptome. The sampled roots separated in two different root types, thereafter named developing storage roots (DSR) or non-bulked roots (NBR) for the respective timepoint (DSR30, DSR38, DSR60, NBR30, NBR38 and NBR60). The analysis indicated that the sampled root types were rather similar on their transcriptional level at 30 dap but became more different in later stages (Fig. 2A). Only 90 of 3790 differently regulated genes (DEGs) were specific for timepoint 30 dap (Fig. 2B).

Most transcriptional changes were observed between the two root types at 38 dap with more than 2000 genes being specifically differently regulated at this timepoint (Fig. 2B). This fitted the increasing visual distinction and onsetting secondary growth at 38 dap. Therefore we focused our analysis on the remaining comparisions containing developing storage roots (DSR38/NBR38, DSR60/NBR60, DSR38/DSR30 & DSR60/DSR38). The up- and downregulated genes were used for KEGG pathway enrichment (Table S2 at Dryad).

This resulted in three significantly enriched pathways of particular interest: "Sucrose and starch metabolism", "Amino sugar and nucleotide metabolism", and "Plant hormone signal transduction" in the significantly upregulated genes of DSR38/NBR38, DSR60/NBR60 and DSR60/DSR38 (Fig. 2C).

The pathway "Sucrose and starch metabolism" (Table S3 at Dryad, sheet 1) was enriched in upregulated genes of DSR60/NBR60 and DSR60/DSR38. Transcriptional upregulation of starch biosynthesis during storage root development is expected considering the high starch content of cassava tuberous roots at stage 60 dap (Fig. 1B). The "Amino sugar and nucleotide sugar metabolism" (Table S3 at Dryad, sheet 2) pathway was enriched in upregulated genes of DSR38/NBR38 and DSR60/NBR60. This pathway included the biosynthesis of diffferent ADP, GDP- and UDP-sugars necessary for primary and secondary cell wall synthesis, which had their highest epression in SRs at 38 dap. The enrichment at the timepoint 60 dap was mainly caused by some overlapping genes with the “Sucrose and starch metabolism” pathway, as well as different α-GLUCOSIDASE and CHITINASES. Fewer cell wall metabolism genes were observed in DSR60/NBR60.

Genes contained in "Plant hormone signal transduction" (Table S3 at Dryad, sheet 3) were solely enriched in DSR38/NBR38, indicating that extensive developmental changes occured around the 38 dap timepoint. Most notably, genes involved in auxin- and cytokinin-signaling were upregulated in DSR compared to NBR. The significant enrichment of the “Phagosome” (Table S3 at Dryad, sheet 4) in DSR38/NBR38 was caused by different *TUBULIN and RAC/RHO GTPase* genes. Although these gene groups have many different functions, their regulation might reflect a high activity of the cytoskeleton during periods of cell division and cellular restructuring.

Regulation of starch and cell wall sugar biosynthesis

Starch and cell wall biosynthesis both compete for monosaccharide building blocks. This was also reflected in the differential expression of genes involved in either pathway (Fig. 3). Genes involved in cell wall formation were generally upregulated in DSR38/NBR38, while genes involved in starch synthesis were generally upregulated in DSR60/NBR60.

UDP-glucose (UDP-glc) is a key substrate in the biosynthesis of most secondary cell wall sugars, especially in form of UDP-glucuronic acid (UDP-glcA). This interconversion is catalyzed by the enzyme UDP-GLUCOSE DEHYDROGENASE (UGDH) (Tenhaken and Thulke, 1996). One *UGDH* gene (Manes.14G084200) showed the most characteristic expression pattern in relation to the KEGG pathway analysis (Fig. 2C) by being strongly upregulated in DSR38/NBR38 and having next to no expression in DSR60. UGDH catalyzes the first non-reversible reaction in hemicellulose synthesis and lack of the enzyme causes severe defects in secondary cell wall and pectin deposition as result of a low UDP-glcA amount (Reboul *et al.*, 2011). UDP-glcA serves as substrate for UDP-xylose synthesis through the enzymes UDP-XYLOSE SYNTHASE (UXS) or UDP-APIOSE/UDP-XYLOSE SYNTHASE (AXS) (Kuang *et al.*, 2016). Two *UXS* genes (Manes.04G032900 & Manes.11G132500) were upregulated at

DSR38/NBR38 and either not upregulated in DSR60/NBR60 or downregulated in DSR60/DSR38. Xylose forms the backbone of xylans, the main polysaccharide in hemicellulose, which biosynthesis is not fully understood yet (Pauly *et al.*, 2013). However, CELLULOSE SYNTHASE-LIKE D (CSLD) enzymes partake in this process (Bernal *et al.*, 2007). One *CSLD* gene (Manes.05G000900) was solely upregulated in DSR60/NBR60. These genes also play a role in correct meristem morphogenesis (Yang *et al.*, 2016). Plants use UDP-glcA to produce the main pectin subunit, UDP-galacturonic acid (UDP-galA), via the enzyme UDP-GLUCURONIC ACID EPIMERASE (GAE) (Gu and Bar-Peled, 2004). Pectin itself is in part synthesized from UDP-galA through GALACTURONOSYL TRANSFERASE (GAUT) enzymes (Atmodjo *et al.*, 2011). Five *GAUT* genes were differentially expressed and showed a similar trend to the other nucleotide sugar biosynthesis genes (Manes.02G085400, Manes.03G122300, Manes.09G119300, Manes.14G088700 & Manes.15G076900). Pectins are part of the primary cell wall that exist in all cells. Generally speaking, nucleotide sugar biosynthesis genes showed an upregulation in DSR38/NBR38 and a downregulation in DSR60/DSR38. This is especially true for genes directly using monosacharides UDP-glc and fructose-6-phosphate. This gene expression pattern was likely the result of different cellular composition of the different samples with 38 dap samples containing a higher ratio of cells displaying a secondary cell wall and samples of 60 dap containing more parenchyma cells.

Genes involved in branching off sugars from sucrose breakdown towards secondary cell wall sugars were downregulated again at stage DSR60 (Fig. 3). At this stage, starch biosynthesis genes were strongly expressed and were upregulated between stage 38 and 60 dap (Fig. 3). This fits with the strong increase in starch measured at 60 compared to 38 dap (Fig. 1B). Notably, a plastidic *PHOSPHOGLUCOMUTASE* (*PGM*) gene (Manes.14G031100) was strongly upregulated in DSR60/DSR38 or DSR60/NBR60 indicating that more glucose-6-phosphate (g-6-p) was converted to glucose-1-phosphate (g-1-p) (Periappuram *et al.*, 2000) in established storage roots. In addition, one *GLUCOSE-6-PHOSPHATE/PHOSPHATE TRANSLOCATOR (GPT;* Manes.16G010700*)* was strongly upregulated in the same way as *PGM*, indicating g-1-p production directly in amyloplasts. G-1-p is the substrate for ADP-GLUCOSE PYROPHOSPHORYLASE (AGPase), which forms ADP-glucose, the substrate for starch biosynthesis. Five genes encoding for AGPase subunits were differentially expressed during root bulking, of which two small subunits (Manes.12G067900 & Manes.18G019650) and one large subunit (Manes.11G085500) were upregulated at DSR60/DSR38. The production of amylose is mainly catalyzed by the enzyme GRANULE-BOUND STARCH SYNTHASE (GBSS) (Kuipers *et al.*, 1994). Cassava GBSS was upregulated at DSR60/NBR60 with a non-significant upregulation in DSR60/DSR38 (Manes.02G001000). Both differentially expressed *SS* genes, one *SS1* (Manes.01G184000) and one *SS2* (Manes.02G046900), encode for plastid-localized enzymes and were upregulated in DSR60/DSR38. *SS1* was shown to be a major determinant of starch synthesis (Delvallé *et al.*, 2005). The other important enzyme in amylopectin synthesis, STARCH BRANCHING ENZYME (BE) that produces the characteristic α-1-6-glucosyl branches (Guan *et al.*, 1995) also showed upregulated genes in DSR60/NBR60 and DSR60/DSR38 (Manes.05G133800, Manes.08G022400 & Manes.S024960). Furthermore, *STARCH PHOSPHORYLASES* (*PHS*), that catalyze the reversible phosphorylation of starch to g-1-p (Hanes and Blackman, 1940), were upregulated in similar manner to the other starch genes. These consist of four plastidic (Manes.02G052280, Manes.02G052360, Manes.02G052520 & Manes.02G052600) and two cytosolic forms of *PHS* (Manes.02G122500 & Manes.17G049200). The presence of active *PHS* genes together with starch biosynthesis genes speaks for their role in starch remodelling rather then breakdown. Especially

because other starch catabolic genes, like *α-AMYLASES* (*αAMY*; Manes.18G037100) and *β-AMYLASES* (*βAMY*; Manes.03G155800, Manes.12G078500 & Manes.15G060100) showed the opposite trend by being downregulated in DSR60/DSR38 or DSR60/NBR60. The same trend was seen for four genes annotated as *TREHALOSE-6-PHOSPHATE SYNTHASE/PHOSPHATASE* (*TPS/TPP*) genes (Manes.01G198900, Manes.05G087900, Manes.06G103000 & Manes.15G098800). Different TPS/TPP proteins can catalyze either the production of trehalose-6-phosphate (t-6-p) from UDP-glc or the back reaction, while others are not catalytically active and only have regulatory purpose (Fichtner *et al.*, 2020) making an interpretation of these DEGs difficult.

One *VACUOLAR INVERTASE* (Manes.01G076500) and two *CELL WALL INVERTASES* (*cwINV*; Manes.03G049200 & Manes.11G025400) were downregulated in a similar fashion. Reduction in *cwINV* expression fits to the observation that cassava switches from a apoplasmic mode of transport in non-bulked roots to a symplasmic mode of transport in tuberous roots (Mehdi *et al.*, 2019). Tuberous roots were shown to possess high SUCROSE SYNTHASE (SUS) activity (Mehdi *et al.*, 2019). Indeed, the main SUS genes of tuberous roots (Manes.01G221900, Manes.03G044400, Manes.16G090600) were highly expressed, however, their transcription was not significantly regulated between the different root samples. Three less expressed *SUS* genes, consisting of two *SUS5* genes (Manes.01G123800 & Manes. 02G081500) and one *SUS6* gene (Manes.14G107800) were downregulated in DSR60/DSR38 and their proteins are only minor contibutors to the total SUS protein amount in tuberous roots (Mehdi *et al.*, 2019). Similar to *SUS*, *UDP-GLUCOSE PYROPHOSPHORYLASE (UGPase),* the enzyme that interconverts UDP-glc and g-1-p, was highly expressed but not significantly regulated between the samples. Transcriptional upregulation of *SUS* and *UGPase* was demonstrated in very early stages of potato tuber formation (Zrenner et al., 1993; Ferreira and Sonnewald, 2012) but could not be demonstrated for cassava tuberous roots in this study, indicating either an even earlier onset of *SUS* expression or posttranscriptional regulation.

Auxin signaling and vascular cambium establishment

Secondary growth in roots is accomplished through asymmetric cell division of stem cells. Previous studies on the morphology of cassava plants showed that adult storage roots continuously grow from a single vascular cambium ring, which resembles the secondary growth of model plants like *A. thaliana* or poplar.

In Arabidopsis, the vascular cambium is induced by an initial auxin maximum causing the expression of *CLASS III HOMEODOMAIN LEUCINE ZIPPER TRANSCRIPTION FACTORS* (*HD-ZIP IIIs*) in procambium and pericycle cells that are connected to primary xylem cells (Smetana et al., 2019). In this study, one *PHABULOSA* (*PHB*) homologue (Manes.06G055000) was significantly upregulated in DSR38/NBR38 and DSR60/NBR60 (Fig. 4). As expected, this coincides with an enrichment of hormone signal transduction (Fig. 2C) in DSR38/NBR38, of which most DEGs are part of the auxin signal transduction pathway (Fig. 4, orange). These included two differentially expressed *AUXIN RESISTANT 1* (*AUX1*) genes (Manes.07G127400 & Manes.08G090700). *AUX1* encodes an auxin influx carrier and takes part in auxin transport into target tissues during gravitropism and root development (Yang *et al.*, 2006; Band *et al.*, 2014). After reception, auxin acts by inducing proteolysis of AUXIN RESISTANT/INDOLE-3-ACETIC ACID INDUCIBLE (AUX/IAA) proteins. This leads to the activation of AUXIN RESPONSE FACTORS (ARFs) at the protein level. Here, four *AUX/IAA* genes were upregulated in DSR38/NBR38 (Manes.09G152700, Manes.11G051200, Manes.16G112900 &

Manes.16G122601), while no ARFs showed differential expression between the two tissues. However, eleven *SMALL AUXIN UPREGULATED RNA* (*SAUR*) encoding genes were upregulated (Manes.04G080700, Manes.04G081500, Manes.04G082200, Manes.05G149166, Manes.05G149400, Manes.05G191200, Manes.09G064000, Manes.11G068170, Manes.11G091848, Manes.18G015150 & Manes.S086000). As the name suggests, *SAUR* genes are upregulated upon auxin signaling and are commonly used as indicators for an active auxin response (McClure and Guilfoyle, 1987; McClure and Guilfoyle, 1989; Esmon *et al.*, 2006). One *GRETCHEN HAGEN 3/INDOLE-3-ACETIC ACID-AMIDO SYNTHASE (GH3.1)* encoding gene was downregulated in DSR38/NBR38. These genes are usually upregulated in response to auxin. They catalyze the conjugation of indole-3-acetic acid with amino acids to inactivate the phytohormone. *A. thaliana GH3.1* mutants show hypersensitive auxin responses (Staswick *et al.*, 2005).

Other genes that were expressed along with *PHB* included important genes during vascular tissue development such as the receptor *PHLOEM INTERCALATED WITH XYLEM* (*PXY*) (Manes.14G037000) and its ligands *CLAVATA3/ESR-RELATED 41* (*CLE41*) or *CLE44* (Manes.12G052002 & Manes.13G045100). In *A. thaliana* roots, *PXY* is controlled through *HD-ZIPIII* activity and, together with *CLE41/44,* retains stem cell activity in the vascular cambium (Fisher and Turner, 2007; Hirakawa *et al.*, 2008; Etchells and Turner, 2010; Smetana *et al.*, 2019) through *WUSCHEL-RELATED HOMEOBOX 4* (*WOX4*) and subsequent *WOX14* expression. (Hirakawa *et al.*, 2010; Etchells *et al.*, 2013). However, no *WOX4* gene was differentially expressed and no gene in the current annotation file was annotated as *WOX14*. Nevertheless, the closest *AtWOX14* homologue (Manes.05G124300) was significantly upregulated in DSR38/NBR38 (Fig. S1 at Dryad digital repository). Further important genes in vascular cambium establishment, maintenance and regulation of differentiation involve *KNOTTED-LIKE HOMEOBOX* (*KNOX*) and *BELLRINGER* (*BEL*) factors. Three *KNOTTED-LIKE FROM ARABIDOPSIS THALIANA 1* (*KNAT1*) homologues in this data set (Manes.05G184900, Manes.18G051700 & Manes.18G052901) were significantly upregulated in DSR38/NBR38 and DSR60/NBR60, but showed much higher expression at DSR60 than DSR38. KNOX proteins function as hetero dimers together with BEL-factors (Hay and Tsiantis, 2010). KNAT1 is known to interact with the functional paralogues PENNYWISE (PNY) and POUND-FOOLISCH (PNF) (Smith *et al.*, 2004; Ragni *et al.*, 2008), both of which have homologues in cassava that showed the same expression pattern as *KNAT1* (Manes.09G097500; Manes.11G148000). These interaction pairs are known to repress the expression of boundary genes *BLADE-ON-PETIOLE 1* (*BOP1*) or *BOP2*, as is the case here with one *BOP2* (Manes.08G056500) homologue being downregulated in DSR (Woerlen *et al.*, 2017). Despite that, this *BOP2* gene was most highly downregulated at DSR38/NBR38 and the *KNAT1* genes had their highest expression at 60 dap. Downstream factors of *BOP2* showed a similar pattern to the boundary gene. These included a homologue of the flowering gene *APETALA1/AGAMOUS-like 7* (*AP1/AGL7*; Manes.01G103200). Another flowering time gene, *AGL20* (Manes.05G041900), was downregulated in a similar manner. Other crop species like potatoes or onions utilize an adapted flowering pathway for storage organ initiation with homologous of the *FLOWERING LOCUS T* (*FT*) serving as a mobile induction signal but also being expressed in the storage organ (Navarro *et al.*, 2011; Lee *et al.*, 2013; Abelenda *et al.*, 2014). No expression of *FT* homologues was found in any samples. The cassava storage root is a perennial organ that is not linked to reproduction. This implies a different regulation in comparison to vegetative reproduction organs, i.e. potatoes or onion bulbs. In addition, lack of flowering-time genes has been linked to perennial growth (Melzer *et al.*, 2008). *KNAT1* was associated with the expression of the boundary gene *LOB DOMAIN-CONTAINING*

PROTEIN (LBD) 4 (Zhang et al., 2019). One gene was upregulated in DSR38/NBR38 and DSR60/NBR60 (Manes.06G173400). *LBD4* takes part in keeping the procambium-phloem boundary together with *PXY* (Smit *et al.*, 2020) and is able to promote the expression of *PETAL LOSS (PTL)* on the phloem side of the vasculature where it restrict expression of *WOX4* to maintain organ boundaries (Zhang et al., 2019). Three PTL genes were upregulated in at least DSR38 versus NBR38 (Manes.10G055600) with two being also upregulated at SR60/NBR60 and DSR60/DSR38 (Manes.07G000300 & Manes.08G021500).

Upregulation of auxin-related transcripts seems to be paralleled by a general downregulation of gibberellin-related transcripts. Changes in gibberellin regulation have been reported during storage organ formation in potato and sweetpotato (Rosin *et al.*, 2003; Singh *et al.*, 2019). With the exception of one upregulated GA20 oxidase (Manes.S084560), all DEGs involved in GA metabolism are downregulated in DSR38/NBR38 or over time in DSR. This includes four *ENT-KAURENE SYNTHASE (KS)* genes (Manes.16G000900, Manes.16G047800, Manes.16G065800, Manes.16G067901), three *GIBBERELLIN-2 OXIDASE (GA2OX)* (Manes.01G231100, Manes.15G121600, Manes.17G070100), three *GIBBERELLIN-3 OXIDASE (GA3OX)* (Manes.04G120200, Manes.11G050500, Manes.16G067700) and one *GIBBERELLIN-20 OXIDASE* (GA20OX) (Manes.05G042300) gene. While the regulation of GA-related genes is likely different depending on the cell type, an overall much lower expression was observed in developing storage roots compared to their non-bulked counterparts.

Finally, the cambium gene *AINTEGUMENTA (ANT)* had two homologues upregulated in DSR38/NBR38 and DSR60/NBR60 (Manes.05G184000 & Manes.18G050000). *ANT* controls the cell proliferation and differentiation with overexpression of the gene in *A. thaliana* causing higher cell number and larger organs without altering the shape of the plant (Mizukami and Fischer, 2000). *ANT* works together with the cell cycle control gene *CYCLIN D3;1 (CycD3;1)* in a cytokinin-dependent manner (Randall *et al.*, 2015). One *CycD3;1* gene (Manes.07G076800) was upregulated in DSR38/NBR38. While, there were no differentially expressed cytokinin biosynthesis genes in our data, some genes in cytokinin signal transduction are upregulated in DSR38/NBR38 or DSR60/NBR60, i.e. *CYTOKININ RECEPTOR 1* like gene (*CRE1*; Manes.15G137400), *ARABIDOPSIS THALIANA RESPONSE REGULATOR 3* (*ARR3*; Manes.18G111900) and *ARABIDOPSIS THALIANA HISTIDINE PHOSPHOTRANSFER PROTEINS* (*AHP;* Manes.04G134100).

Overall, the results of the transcriptome analysis indicated that the developing storage roots underwent extensive cellular restructuring before the storage metabolism was activated. This can be derived from the strong transcriptional activation of genes encoding cell wall-modifying enzymes and hormone-signaling components at stage 38 dap, as well as from the subsequent activation of storage metabolism between 38 and 60 dap. Although many of the developmental genes mentioned above were not significantly regulated within the comparisions of DSR samples, they showed differential expression between NBR and DSR samples, indicating that both tissues underwent a different program during their development. To get a deeper insight into the underlying structural and transcriptional processes happening in developing storage roots and to validate the field results independently, we performed a controlled greenhouse time-course experiment, covering the sampling timepoints of the RNA-seq experiment, as well as additional timepoints. The samples were used for histological analysis and qRT-PCR verification.

Morphological changes during root bulking

Stem sticks of cassava genotype TME7, a genotype closely related to TME419 (Bredeson *et al.*, 2016), were planted in the greenhouse. Potential and developing storage roots emerging from the nodal areas of cassava stem pieces were sampled at seven timepoints (22, 26, 30, 34, 38, 42 and 60 dap) to get a broad line-up of developing storage roots at different ages and developmental stages. Cross-sections of the primary bulking site of every sampled root were taken and the resulting sections stained with toluidine blue solution to be able to group these roots according to their morphology, rather than their sampling timepoint (Fig. 5A-F).

Developing roots were sorted into five developmental stages based on their cellular composition and appearance. Stage one roots had a typical primary root morphology (Fig. 5A) and were observed in plants at 22 or 26 dap. They contained a star-shaped central cylinder encased in an endodermis. Inside the central cylinder were alternating primary phloem and xylem cells with a procambium in between (indicated by a small layer of dividing cells).

The radial symmetry of the developing storage root was established between stage two and four (Fig. 5B-D). In stage two (Fig. 5B), the shape of the xylem and phloem tissue was less organized compared to stage one, indicating ongoing asymmetric cell division of the procambium that produces new phloem and xylem cells. The endodermis got pushed towards the outside, which lead to a circular shape of the central cylinder. The cortex cells were still more or less intact. Stage three nodal roots showed further increase in size of the central cylinder (Fig. 5C). The cambium was highly active and had a larger diameter than in previous stage albeit not being of radial shape yet. The newly formed cells were mostly lignified xylem cells, as indicated by the blue coloring of the newly formed cells towards the center. This fits the strong transcription activation of cell wall-related genes in field-grown plants at timepoint 38. The phloem tissue did not increase much in comparison to younger roots. The endodermis was still intact, but the cortex was severely squashed towards the rhizodermis. The first vascular rays appeared but were hard to pinpoint at this stage. No starch was formed up until now (Fig. 5G-I). Stage four (Fig. 5D) developing storage root were marked by disbandment of the endodermis and an annular shape of the inner xylem as well as an overall radial shape of the root. The cortex was completely missing and the rhizodermis was displaced by a periderm at this stage. The root did not yet grow in diameter. However, the periderm gave it a visible brown coloring compared to the pale white of young roots. Furthermore, starch storage began in this phase of root development as indicated by Lugol staining (Fig. 5J). The stain was visible in the inner xylem cells adjacent to the vascular ray and the ray cells themselves, but most of the starch was still stored in phloem parenchyma cells. Similar to the field samples (Fig. 1A) a strong increase in starch is only measurable in established storage roots approximately 60 dap (Fig. S2A at Dryad digital repository). The color change between stage three and four was the main factor in root sampling for the transcriptome experiment making this the likely developmental range of developing storage roots at 38 dap. Transcriptional changes at this timepoint were predominately characterized by higher expression of secondary cell wall synthesis genes in tuberous roots. Secondary cell walls are solely deposited in differentiated sclerenchyma cells (Zhong *et al.*, 2019). These include lignified xylem cells, which were strongly produced at this developmental stage (Fig. 5C-D). The number of meristematic cells increased, which explains the high expression of cambium genes, i.e. *PXY* (Etchells and Turner, 2010). Furthermore, the procambium developed into the ring-shaped vascular cambium

during this time. This coincided with higher expression of auxin signal transduction genes and *HD-ZIPIII*.

The more established storage roots (stage five; (Fig. 5E-F)) were easily identified on a macroscopic level due to an increase in lateral size. The vascular cambium mostly produced xylem parenchyma cells that were rapidly filled with starch, which is indicated by even the youngest cells being stained by the Lugol solution (Fig. 5K). This coincided with downregulation of secondary cell wall genes, upregulation of starch biosynthesis genes, high amounts of starch (Fig. 1B; Fig. 5K; Fig. S2 at Dryad digital repository), as well as strong upregulation of *KNOX* and *BEL* genes *KNAT1*, *PNY* and *PNF.* In *A. thaliana*, *KNAT1* is able to regulate the differentiation of xylem fibers in secondary meristems (Byrne *et al.*, 2002; Mele *et al.*, 2003; Liebsch *et al.*, 2014) through regulation of GA signaling (Hay *et al.*, 2002; Bolduc and Hake, 2009; Felipo-Benavent *et al.*, 2018). In roots and hypocotyls of *A. thaliana, KNAT1* promotes differentiation (Liebsch *et al.*, 2014), while its overexpression in aerial parts of the plant lead to fewer lignified cells (Mele *et al.*, 2003). A function that is similar in poplar trees (Groover *et al.*, 2006). In other root and tuber crops, *KNOX/BEL* modules play a necessary role in the development of starchy storage organs. Sweet potatoes show similar expression levels of a *BEL1* gene in late developmental stages compared to *PNF* in this study (Dong *et al.*, 2019), which goes hand-in-hand with low GA signaling causing lower amounts of lignified cells to be produced (Singh *et al.*, 2019). In potatoes, the *KNOX* gene *POTATO HOMEOBOX 1* (*POTH1*) acts in a similar manner together with the BEL-factor *BEL5* (Rosin *et al.*, 2003; Banerjee *et al.*, 2006; Lin *et al.*, 2013). Our study suggests that the low amount of lignified xylem cells was related to high *KNAT1*/*PNF* and/or *KNAT1*/*PNY* activity in cassava tuberous root after establishment of the vascular cambium.

Independent qPCR validation of observed transcriptional changes

To validate and further elucidate the results of the RNA-seq analysis, a set of genes was chosen to represent the most important pathways and regulatory networks (Table 1; Primer list in Table S4 at Dryad) found regulated during storage root development in the transcriptome analysis. The expression was analyzed via qRT-PCR on the different developing storage root stages. The respective morphology and corresponding root stage were microscopically confirmed for every root.

Table 1. Selected genes for qRT-PCR validation.

Abbr.	Name	Identifier
AGL20	*AGAMOUS-like 20*	Manes.01G263500
ANT	*AINTEGUMENTA*	Manes.05G184000
AUX1	*AUXIN RESISTANT 1*	Manes.07G127400
BOP2	*BLADE-ON-PETIOLE*	Manes.08G056500
CLE41	*CLAVATA3/ESR-RELATED 41*	Manes.13G045100
GH3.1	*GRETCHEN HAGEN 3.1/INDOLE-3-ACETIC ACID-AMIDO SYNTHASE*	Manes.13G116000
GID1B	*GIBBERELLIN INSENSITIVE DWARF 1B*	Manes.01G212300
KNAT1	*KNOTTED-LIKE FROM ARABIDOPSIS THALIANA 1*	Manes.05G184900
LBD4	*LOB DOMAIN-CONTAINING PROTEIN 4*	Manes.06G173400
PMI	*PHOSPHOMANNOSE ISOMERASE*	Manes.02G069000
PGM	*PHOSPHOGLUCOMUTASE*	Manes.14G031100
PHB	*PHABULOSA*	Manes.06G055000
PHS	*STARCH PHOSPHORYLASE*	Manes.02G052600
PNF	*POUND-FOOLISH*	Manes.11G148000
PNY	*PENNYWISE*	Manes.09G097500
PXY	*PHLOEM INTERCALATED WITH XYLEM*	Manes.14G037000
TPS	*TREHALOSE-6-PHOSPHATE SYNTHASE/PHOSPHATASE*	Manes.06G103000
UGDH	*UDP-GLUCOSE DEHYDROGENASE*	Manes.14G084200
SUS	*SUCROSE SYNTHASE*	Manes.03G044400
UGPASE	*UDP-GLUCOSE PYROPHOSPHORYLASE*	Manes.02G080600

The *BEL*-factors *PNY* and *PNF* were strongly upregulated in stage five developing storage roots with a slight upward trend from stage one to four (Fig. 6). *PNF* expression was especially high with a 40-fold upregulation in the more established developing storage roots in comparison to stage one. A very similar trend is shown in the expression of *KNAT1*. The expression of these three genes correlated with the expression of starch genes *PGM* and *PHS*, but also with a production of a high number of xylem parenchyma cells (Fig. 5K).

The boundary genes behaved as predicted. *BOP2* expression showed a downward trend with especially low expression at stage five, which coincided with high expression of the *KNAT1/BEL* module. They also showed a significant negative correlation (Fig. 6, top left.). *LBD4*, while not being upregulated throughout root bulking, was expressed similarly to the transcriptome data set at every stage.

PXY expression was detectable in every stage of root bulking. However, the expression dropped down at stage three and went up in later stages again. This was highly correlated with the expression of *PHB*, which supports the hypothesis shown in Fig. 4 that *PXY* expression in cassava is dependent on an auxin signal inducing *PHB* expression, even though the change in the *HD-ZIPIII* gene is rather minute in comparison to *PXY* (Smetana *et al.*, 2019; Zhang *et al.*, 2019). This expression pattern was exactly contrary to the expression levels of *GID1B* and *TPS* as well as *GH3.1*, *PMI* and *BOP2* to a lesser extent. This coincided with deposition of lignified xylem cells by the vascular cambium between stage three and four (Fig. 5C-D) and with a comparably small upregulation of the GA receptor *GID1B*, which might indicated a short GA signaling spike for the production of lignified cells. The starch biosynthesis genes *PHS* and *PGM* were strongly expressed at stage five in developing

storage roots and have close to no expression at the other stages. This fits the histological analysis, where starch was mainly produced at stage five with negligible amounts in stage four and no starch in stage one to three (Fig. 5G-L, Fig. S2A at Dryad digital repository). Expression of these starch genes varied greatly within stage five roots but did correlate with the starch content of the particular roots (Fig. S2B-C at Dryad digital repository). *AGL20* is strongly downregulated between stage four and five, showing strong opposite behavior to the *KNOX/BEL* and *PGM/PHS* genes. *ANT, CLE41* and *AUX1* increased in expression with advancing development. Similar to the transcriptomic results, *SUS* and *UGPase* did not exceed a |log2FC| of 1 between the developing storage root stages.

The gene expression results obtained from independent samples with an independent method support the hypothesis formed through the transcriptome analysis, since the genes clustered in distinct groups (Fig. 6, top left) or otherwise resembled the transcriptional profile shown in Fig. 3 and 4. *GID1B, TPS, BOP2* and *GH3.1* formed a cluster as expected and were more highly expressed in early stages of nodal roots (Fig. 6, cluster 1). The proposed auxin signaling genes (*AUX1, PHB* and *PXY*) were tightly correlated with each other, as well as with *ANT* (Fig. 6, cluster 2). Starch biosynthesis genes were only strongly expressed in stage five roots together with the *KNOX/BEL* genes (Fig. 6, cluster 6) in accordance with the transcriptome dataset.

Conclusion

This study investigated the transcriptional and morphological changes occuring during early storage root development. We show that lateral size increase in storage roots was accomplished through establishment of a singular vascular cambium and subsequent deposition of non-lignified parenchyma cells. Early storage root development was marked by production of lignified cells in the central cylinder. This coincided with the strong expression of important secondary cell wall biosynthesis genes, i.e. *UGDH*, *GAE, UXS* and *GAUT*. The same genes were downregulated in later stages where starch biosynthesis is the dominantly active pathway. Starch biosynthesis began only after the establishment of the vascular cambium, after which mainly xylem parenchyma cells were produced. We demonstrate that this was accompanied by strong transcriptional upregulation of plastid-localized starch biosynthesis genes like *PGM*, *AGPase*, *GBSS, SS* and *BE* genes. The vascular cambium itself was formed through a transcriptionally strong auxin response correlated with expression of a *HD-ZIPIII* gene and subsequent expression of *PXY*, *CLE41*/*44* and *WOX14*. The formation of parenchyma rather than sclerenchyma cells was accompanied by high expression of the *KNOX*/*BEL* genes *KNAT1, PNY, PNF*, highlighting their importance for xylem parenchyma function.

While this study provides a groundwork for a lesser-known crop species, it also raises many questions to be answered. For instance, direct genetic alteration of different developmental regulators of storage root expansion and storage parenchyma formation is highly interesting. Understanding the role of *KNOX/BEL* factors and the role of different hormones in the suppression of secondary cell wall biosynthesis in storage parenchyma cells should yield useful information for further advances in cassava.

Acknowledgements

We thank David Pscheidt, Michaela Brock, Anetor Omonuwa and Brandon Harris for excellent technical assistance. We thank Rabih Mehdi for his help with the cassava root cross-sections and Peter Iluebbey and the IITA Cassava Breeding Unit for logistic support during the field work. We thank the Bill and Melinda Gates Foundation for funding this research through the grant INV-008053 "Metabolic Engineering of Carbon Pathways to Enhance Yield of Root and Tuber Crops" provided to Prof. Dr. Uwe Sonnewald.

Author contribution

D.R. processed and evaluated the transcriptomic data, performed qRT-PCR and histological experiments. J.M.C.G supervised the bioinformatical processing of the raw data. A.G., L.S. and A.V.C. performed the field experiment and generated the transcriptomic data. P.K and E.N. contributed the metabolite data. All authors contributed to experimental design and interpretation. U.S. and W.Z. supervised the work. D.R. and W.Z wrote the manuscript with contributions of all authors.

Data availability statement

The data for this study has been deposited in the European Nucleotide Archive (ENA) at EMBL-EBI under accession number PRJEB41121. Supplementary data has been deposited in Dryad digital repository under https://doi.org/10.5061/dryad.0cfxpnw0t.

References

Abelenda JA, Navarro C, Prat S. 2014. Flowering and tuberization: a tale of two nightshades. Trends in Plant Science 19, 115-122.

Agusti J, Herold S, Schwarz M*, et al.* 2011. Strigolactone signaling is required for auxin-dependent stimulation of secondary growth in plants. Proceedings of the National Academy of Sciences **108**, 20242-20247.

Atmodjo MA, Sakuragi Y, Zhu X, Burrell AJ, Mohanty SS, Atwood III JA, Orlando R, Scheller HV, Mohnen D. 2011. Galacturonosyltransferase (GAUT)1 and GAUT7 are the core of a plant cell wall pectin biosynthetic homogalacturonan:galacturonosyltransferase complex. Proceedings of the National Academy of Sciences **108**, 20225-20230.

Band LR, Wells DM, Fozard JA*, et al.* 2014. Systems analysis of auxin transport in the *Arabidopsis* root apex. The Plant Cell **26**, 862-875.

Banerjee AK, Chatterjee M, Yu Y, Suh S-G, Miller WA, Hannapel DJ. 2006. Dynamics of a mobile RNA of potato involved in a long-distance signaling pathway. The Plant Cell **18**, 3443-3457.

Bennett MJ, Marchant A, Green HG, May ST, Ward SP, Millner PA, Walker AR, Schulz B, Feldmann KA. 1996. *Arabidopsis AUX1* gene: a permease-like regulator of root gravitropism. Science **273**, 948-950.

Bernal AJ, Jensen JK, Harholt J*, et al.* 2007. Disruption of *AtCSLD5* results in reduced growth, reduced xylan and homogalacturonan synthase activity and altered xylan occurrence in *Arabidopsis*. The Plant Journal **52**, 791-802.

Biemelt S, Tschiersch H, Sonnewald U. 2004. Impact of altered gibberellin metabolism on biomass accumulation, lignin biosynthesis, and photosynthesis in transgenic tobacco plants. Plant Physiology **135**, 254-265.

Björklund S, Antti H, Uddestrand I, Moritz T, Sundberg B. 2007. Cross-talk between gibberellin and auxin in development of *Populus* wood: gibberellin stimulates polar auxin transport and has a common transcriptome with auxin. The Plant Journal **52**, 499-511.

Bolduc N, Hake S. 2009. The maize transcription factor KNOTTED1 directly regulates the gibberellin catabolism gene *ga2ox1*. The Plant Cell **21**, 1647-1658.

Bredeson JV, Lyons JB, Prochnik SE, *et al.* 2016. Sequencing wild and cultivated cassava and related species reveals extensive interspecific hybridization and genetic diversity. Nature Biotechnology **34**, 562-570.

Byrne ME, Simorowski J, Martienssen RA. 2002. *ASYMMETRIC LEAVES1* reveals knox gene redundancy in *Arabidopsis*. Development **129**, 1957-1965.

Campilho A, Nieminen K, Ragni L. 2020. The development of the periderm: the final frontier between a plant and its environment. Current Opinion in Plant Biology **53**, 10-14.

Carraro N, Tisdale-Orr TE, Clouse RM, Knöller AS, Spicer R. 2012. Diversification and Expression of the PIN, AUX/LAX, and ABCB Families of Putative Auxin Transporters in *Populus*. Frontiers in Plant Science **3**.

Carvalho LJCB, Filho JF, Anderson JV, Figueiredo PG, Chen S. 2018. Storage Root of Cassava: Morphological Types, Anatomy, Formation, Growth, Development and Harvest Time. *Cassava*: IntechOpen.

Chaweewan Y, Taylor N. 2015. Anatomical assessment of root formation and tuberization in cassava (*Manihot esculenta* Crantz). Tropical Plant Biology **8**, 1-8.

Delvallé D, Dumez S, Wattebled F, *et al.* 2005. Soluble starch synthase I: a major determinant for the synthesis of amylopectin in *Arabidopsis thaliana* leaves. The Plant Journal **43**, 398-412.

Ding Z, Fu L, Tie W, Yan Y, Wu C, Dai J, Zhang J, Hu W. 2020. Highly dynamic, coordinated, and stage-specific profiles revealed by multi-omics integrative analysis during cassava tuberous root development. Journal of Experimental Botany, eraa369.

Dobin A, Davis CA, Schlesinger F, Drenkow J, Zaleski C, Jha S, Batut P, Chaisson M, Gingeras TR. 2012. STAR: ultrafast universal RNA-seq aligner. Bioinformatics **29**, 15-21.

Dong T, Zhu M, Yu J, Han R, Tang C, Xu T, Liu J, Li Z. 2019. RNA-Seq and iTRAQ reveal multiple pathways involved in storage root formation and development in sweet potato (*Ipomoea batatas* L.). BMC Plant Biology **19**, 136.

Eriksson ME, Israelsson M, Olsson O, Moritz T. 2000. Increased gibberellin biosynthesis in transgenic trees promotes growth, biomass production and xylem fiber length. Nature Biotechnology **18**, 784-788.

Esmon CA, Tinsley AG, Ljung K, Sandberg G, Hearne LB, Liscum E. 2006. A gradient of auxin and auxin-dependent transcription precedes tropic growth responses. Proceedings of the National Academy of Sciences of the United States of America **103**, 236-241.

Etchells JP, Provost CM, Mishra L, Turner SR. 2013. WOX4 and WOX14 act downstream of the PXY receptor kinase to regulate plant vascular proliferation independently of any role in vascular organisation. Development **140**, 2224-2234.

Etchells JP, Turner SR. 2010. The PXY-CLE41 receptor ligand pair defines a multifunctional pathway that controls the rate and orientation of vascular cell division. Development **137**, 767-774.

Felipo-Benavent A, Úrbez C, Blanco-Touriñán N, Serrano-Mislata A, Baumberger N, Achard P, Agustí J, Blázquez MA, Alabadí D. 2018. Regulation of xylem fiber differentiation by gibberellins through DELLA-KNAT1 interaction. Development **145**, dev164962.

Ferreira SJ, Sonnewald U. 2012. The mode of sucrose degradation in potato tubers determines the fate of assimilate utilization. Frontiers in Plant Science **3**.

Fichtner F, Olas JJ, Feil R, Watanabe M, Krause U, Hoefgen R, Stitt M, Lunn JE. 2020. Functional features of TREHALOSE-6-PHOSPHATE SYNTHASE1, an essential enzyme in *Arabidopsis*. The Plant Cell **32**, 1949-1972.

Firon N, LaBonte D, Villordon A*, et al.* 2013. Transcriptional profiling of sweetpotato (*Ipomoea batatas*) roots indicates down-regulation of lignin biosynthesis and up-regulation of starch biosynthesis at an early stage of storage root formation. BMC Genomics **14**, 460.

Fischer U, Kucukoglu M, Helariutta Y, Bhalerao RP. 2019. The dynamics of cambial stem cell activity. Annual Review of Plant Biology **70**, 293-319.

Fisher K, Turner S. 2007. PXY, a receptor-like kinase essential for maintaining polarity during plant vascular-tissue development. Current Biology **17**, 1061-1066.

Groover AT, Mansfield SD, DiFazio SP, Dupper G, Fontana JR, Millar R, Wang Y. 2006. The *Populus* homeobox gene *ARBORKNOX1* reveals overlapping mechanisms regulating the shoot apical meristem and the vascular cambium. Plant Molecular Biology **61**, 917-932.

Gu X, Bar-Peled M. 2004. The biosynthesis of UDP-galacturonic acid in plants. Functional cloning and characterization of *Arabidopsis* UDP-D-glucuronic acid 4-epimerase. Plant Physiology **136**, 4256-4264.

Guan H, Kuriki T, Sivak M, Preiss J. 1995. Maize branching enzyme catalyzes synthesis of glycogen-like polysaccharide in *glgB*-deficient *Escherichia coli*. Proceedings of the National Academy of Sciences **92**, 964-967.

Hanes CS, Blackman FF. 1940. The reversible formation of starch from glucose-1-phosphate catalysed by potato phosphorylase. Proceedings of the Royal Society of London. Series B - Biological Sciences **129**, 174-208.

Hay A, Kaur H, Phillips A, Hedden P, Hake S, Tsiantis M. 2002. The gibberellin pathway mediates KNOTTED1-type homeobox function in plants with different body plans. Current Biology **12**, 1557-1565.

Hay A, Tsiantis M. 2010. KNOX genes: versatile regulators of plant development and diversity. Development **137**, 3153-3165.

Hirakawa Y, Kondo Y, Fukuda H. 2010. TDIF peptide signaling regulates vascular stem cell proliferation via the *WOX4* homeobox gene in *Arabidopsis*. The Plant Cell **22**, 2618-2629.

Hirakawa Y, Shinohara H, Kondo Y, Inoue A, Nakanomyo I, Ogawa M, Sawa S, Ohashi-Ito K, Matsubayashi Y, Fukuda H. 2008. Non-cell-autonomous control of vascular stem cell fate by a CLE peptide/receptor system. Proceedings of the National Academy of Sciences **105**, 15208-15213.

Immanen J, Nieminen K, Smolander O-P*, et al.* 2016. Cytokinin and auxin display distinct but interconnected distribution and signaling profiles to stimulate cambial activity. Current Biology **26**, 1990-1997.

Kuang B, Zhao X, Zhou C*, et al.* 2016. Role of UDP-glucuronic acid decarboxylase in xylan biosynthesis in *Arabidopsis*. Molecular Plant **9**, 1119-1131.

Kuipers A, Jacobsen E, Visser R. 1994. Formation and deposition of amylose in the potato tuber starch granule are affected by the reduction of granule-bound starch synthase gene expression. The Plant Cell **6**, 43-52.

Lee R, Baldwin S, Kenel F, McCallum J, Macknight R. 2013. *FLOWERING LOCUS T* genes control onion bulb formation and flowering. Nature Communications **4**, 2884.

Li H, Handsaker B, Wysoker A, Fennell T, Ruan J, Homer N, Marth G, Abecasis G, Durbin R, Subgroup GPDP. 2009. The sequence alignment/map format and SAMtools. Bioinformatics **25**, 2078-2079.

Li R, Mock R, Huang Q, Abad J, Hartung J, Kinard G. 2008. A reliable and inexpensive method of nucleic acid extraction for the PCR-based detection of diverse plant pathogens. Journal of Virological Methods 154, 48-55

Liao Y, Smyth GK, Shi W. 2013. featureCounts: an efficient general purpose program for assigning sequence reads to genomic features. Bioinformatics **30**, 923-930.

Liebsch D, Sunaryo W, Holmlund M*, et al.* 2014. Class I KNOX transcription factors promote differentiation of cambial derivatives into xylem fibers in the *Arabidopsis* hypocotyl. Development **141**, 4311-4319.

Lin T, Sharma P, Gonzalez DH, Viola IL, Hannapel DJ. 2013. The impact of the long-distance transport of a BEL1-like messenger RNA on development. Plant Physiology **161**, 760-772.

Livak KJ, Schmittgen TD. 2001. Analysis of relative gene expression data using real-time quantitative PCR and the 2− ΔΔCT method. METHODS **25**, 402-408.

Love MI, Huber W, Anders S. 2014. Moderated estimation of fold change and dispersion for RNA-seq data with DESeq2. Genome Biology **15**, 550.

McClure BA, Guilfoyle T. 1987. Characterization of a class of small auxin-inducible soybean polyadenylated RNAs. Plant molecular biology **9**, 611-623.

McClure BA, Guilfoyle T. 1989. Rapid redistribution of auxin-regulated RNAs during gravitropism. Science **243**, 91-93.

Mehdi R, Lamm CE, Bodampalli RA*, et al.* 2019. Symplasmic phloem unloading and radial post-phloem transport via vascular rays in tuberous roots of Manihot esculenta. Journal of Experimental Botany, **70**, 5559-5573

Mele G, Ori N, Sato Y, Hake S. 2003. The *knotted1*-like homeobox gene *BREVIPEDICELLUS* regulates cell differentiation by modulating metabolic pathways. Genes & development **17**, 2088-2093.

Melzer S, Lens F, Gennen J, Vanneste S, Rohde A, Beeckman T. 2008. Flowering-time genes modulate meristem determinacy and growth form in *Arabidopsis thaliana*. Nature Genetics **40**, 1489-1492.

Mizukami Y, Fischer RL. 2000. Plant organ size control: AINTEGUMENTA regulates growth and cell numbers during organogenesis. Proceedings of the National Academy of Sciences **97**, 942-947.

Navarro C, Abelenda JA, Cruz-Oró E, Cuéllar CA, Tamaki S, Silva J, Shimamoto K, Prat S. 2011. Control of flowering and storage organ formation in potato by FLOWERING LOCUS T. Nature **478**, 119.

Noh SA, Lee HS, Huh EJ, Huh GH, Paek KH, Shin JS, Bae JM. 2010. SRD1 is involved in the auxin-mediated initial thickening growth of storage root by enhancing proliferation of metaxylem and cambium cells in sweetpotato (*Ipomoea batatas*). Journal of Experimental Botany, **61**, 1337-1349.

Obata T, Klemens PAW, Rosado-Souza L*, et al.* 2020. Metabolic profiles of six African cultivars of cassava (*Manihot esculenta* Crantz) highlight bottlenecks of root yield. The Plant Journal, **102**, 1202-1219

Pauly M, Gille S, Liu L, Mansoori N, de Souza A, Schultink A, Xiong G. 2013. Hemicellulose biosynthesis. Planta **238**, 627-642.

Periappuram C, Steinhauer L, Barton DL, Taylor DC, Chatson B, Zou J. 2000. The plastidic phosphoglucomutase from *Arabidopsis*. A reversible enzyme reaction with an important role in metabolic control. Plant Physiology **122**, 1193-1199.

Ragni L, Belles-Boix E, Günl M, Pautot V. 2008. Interaction of *KNAT6* and *KNAT2* with *BREVIPEDICELLUS* and *PENNYWISE* in Arabidopsis Inflorescences. The Plant Cell **20**, 888-900.

Ragni L, Greb T. 2018. Secondary growth as a determinant of plant shape and form. Seminars in Cell & Developmental Biology **79**, 58-67.

Randall RS, Miyashima S, Blomster T*, et al.* 2015. *AINTEGUMENTA* and the D-type cyclin *CYCD3;1* regulate root secondary growth and respond to cytokinins. Biology Open **4**, 1229-1236.

Reboul R, Geserick C, Pabst M, Frey B, Wittmann D, Lütz-Meindl U, Léonard R, Tenhaken R. 2011. Down-regulation of UDP-glucuronic acid biosynthesis leads to swollen plant cell walls and severe developmental defects associated with changes in pectic polysaccharides. Journal of Biological Chemistry **286**, 39982-39992.

Robert HS, Grunewald W, Sauer M, Cannoot B, Soriano M, Swarup R, Weijers D, Bennett M, Boutilier K, Friml J. 2015. Plant embryogenesis requires AUX/LAX-mediated auxin influx. Development **142**, 702-711.

Rosin FM, Hart JK, Horner HT, Davies PJ, Hannapel DJ. 2003. Overexpression of a *KNOTTED*-like homeobox gene of potato alters vegetative development by decreasing gibberellin accumulation. Plant Physiology **132**, 106-117.

Rüscher D, Corral JM, Carluccio AV, Klemens PAW, Gisel A, Stavolone L, Neuhaus E, Ludewig F, Sonnewald U, Zierer W (2021). Auxin signaling and vascular cambium formation enables storage metabolism in cassava tuberous roots. Dryad, Dataset, https://doi.org/10.5061/dryad.0cfxpnw0t

Singh V, Sergeeva L, Ligterink W, Aloni R, Zemach H, Doron-Faigenboim A, Yang J, Zhang P, Shabtai S, Firon N. 2019. Gibberellin promotes sweetpotato root vascular lignification and reduces storage root formation. Frontiers in Plant Science **10**.

Smetana O, Mäkilä R, Lyu M*, et al.* 2019. High levels of auxin signalling define the stem-cell organizer of the vascular cambium. Nature **565**, 485-489.

Smit ME, McGregor SR, Sun H*, et al.* 2020. A PXY-mediated transcriptional network integrates signaling mechanisms to control vascular development in *Arabidopsis*. The Plant Cell **32**, 319-335.

Smith HMS, Campbell BC, Hake S. 2004. Competence to respond to floral inductive signals requires the homeobox genes *PENNYWISE* and *POUND-FOOLISH*. Current Biology **14**, 812-817.

Snow R. 1935. Activation of cambial growth by pure hormones. Nature **135**, 876-876.

Sojikul P, Saithong T, Kalapanulak S, Pisuttinusart N, Limsirichaikul S, Tanaka M, Utsumi Y, Sakurai T, Seki M, Narangajavana J. 2015. Genome-wide analysis reveals phytohormone action during cassava storage root initiation. Plant Molecular Biology **88**, 531-543.

Tenhaken R, Thulke O. 1996. Cloning of an enzyme that synthesizes a key nucleotide-sugar precursor of hemicellulose biosynthesis from soybean: UDP-glucose dehydrogenase. Plant Physiology **112**, 1127-1134.

Utsumi Y, Tanaka M, Utsumi C*, et al.* 2020. Integrative omics approaches revealed a crosstalk among phytohormones during tuberous root development in cassava. Plant Molecular Biology.

Vanderschuren H, Nyaboga E, Poon JS, Baerenfaller K, Grossmann J, Hirsch-Hoffmann M, Kirchgessner N, Nanni P, Gruissem W. 2014. Large-scale proteomics of the cassava storage root and identification of a target gene to reduce postharvest deterioration. The Plant Cell **26**, 1913-1924.

Woerlen N, Allam G, Popescu A, Corrigan L, Pautot V, Hepworth SR. 2017. Repression of *BLADE-ON-PETIOLE* genes by *KNOX* homeodomain protein *BREVIPEDICELLUS* is essential for differentiation of secondary xylem in Arabidopsis root. Planta **245**, 1079-1090.

Yang Y, Hammes UZ, Taylor CG, Schachtman DP, Nielsen E. 2006. High-affinity auxin transport by the AUX1 influx carrier protein. Current Biology **16**, 1123-1127.

Yu G, Wang L-G, Han Y, He Q-Y. 2012. clusterProfiler: an R package for comparing biological themes among gene clusters. OMICS: A Journal of Integrative Biology **16**, 284-287.

Zhang J, Eswaran G, Alonso-Serra J, *et al.* 2019. Transcriptional regulatory framework for vascular cambium development in *Arabidopsis* roots. Nature Plants **5**, 1033-1042.

Zhong R, Cui D, Ye Z-H. 2019. Secondary cell wall biosynthesis. New phytologist **221**, 1703-1723.

Zrenner R, Willmitzer L, Sonnewald U. 1993. Analysis of the expression of potato uridinediphosphate-glucose pyrophosphorylase and its inhibition by antisense RNA. Planta **190**, 247-252.

Figure Legends

Fig. 1 Phenotypic and metabolic characterization of root growth. (**A**) Schematic depiction of root phenotypes at sampling time points 30, 38 and 60 dap. Blue arrows indicate developing storage roots (DSR) and red arrows indicate non-bulked roots (NBR) (**B**) Glucose, fructose, sucrose, starch, protein and total amino acid content of roots identified as (potential) storage roots. (**C**) Individual amino acids measured at different timepoints.

Fig. 2 Basic characterization of the obtained cassava root transcriptomes. (**A**) Principal component analysis on non-bulked roots (NBR) (red) and developing storage roots (DSR) (blue) on log transformed RNAseq data at 30 (circle), 38 (triangle) and 60 dap (square). (**B**) Venn diagrams of differentially expressed genes ($|log2FC| \geq 1$ and FWER ≤ 0.05) on pairwise comparisons (**C**) KEGG pathway enrichment analysis on DEGs of selected pairs. Circles show number of genes in a pathway, the color indicates FWER values and the number in brackets the total number of genes with an annotated KO term within the comparison. Pathways with FWER ≤ 0.05 are shown.

Fig. 3 Overview of carbohydrate-related transcriptional changes between different root stages inferred from differentially expressed genes in the KEGG pathways "Amino sugar and nucleotide sugar metabolism" and "Sucrose and starch metabolism". Heat maps show the log2FC of homologues that are differentially expressed in at least one comparison. Columns from left to right are DSR38/NBR38, DSR60/NBR60 and DSR60/DSR38. Asterisks indicate significant difference in expression with $|log2FC| \geq 1$ and FWER ≤ 0.05. Green rectangles highlight genes with differential expression. Light colored rectangles represent players with no differentially expressed homologues in expression. Red rectangles indicate metabolites.

Fig. 4 Overview on developmental-related changes between different root stages inferred from differentially expressed genes in the KEGG pathway "Plant hormone signal transduction" (green) and from published regulations and interactions (orange). Heat maps show the log2FC of homologues that are differentially expressed in at least one comparison. Columns from left to right are: DSR38/NBR38, DSR60/NBR60 and DSR60/DSR38. Asterisks indicate significant difference in expression with $|log2FC| \geq 1$ and FWER ≤ 0.05. Light colored rectangles represent players with no differentially expressed homologues in expression.

Fig. 5 Histological analysis of cassava storage root development. (A-F) Toluidine blue stained cross-section of different storage root stages. (**A**) Stage one roots show a star shaped central cylinder enclosed by an endodermis. (**B**) Stage two roots have a ring-shaped central cylinder with active cell division depositing of xylem and phloem cells. Endodermis is still intact, and the cortex is still healthy. (**C**) Stage three root with round central cylinder still enclosed in an intact endodermis. Xylem and phloem are irregularly shaped and cortex cells are severely squashed. (**D**) Stage four storage root with radial symmetry and no central cylinder. Rhizodermis is replaced with a periderm and vascular ray cells are visible. Xylem displayed only lignified cells. (**E-F**) Stage five tuberous root with increased lateral size through deposition of xylem parenchyma cells through the vascular

cambium. (**G-K**) Cross-section of storage root from stage one to five stained with Lugol solution. Bars indicate 100µm. Abbreviations: Co, cortex; Ed, endodermis; PP, primary phloem; P, phloem; PX, primary xylem; Pc, procambium; Pd, periderm; Rd, rhizodermis; VC, vascular cambium; VR, vascular ray; X, xylem; XP, xylem parenchyma; XV, xylem vessel.

Fig. 6 Quantitative RT-PCR validation of selected genes regulated during root development. Bars show the mean relative expression normalized to three house-keeping genes (Manes.06G116400 (GAPDH), Manes.06G058300 (HDD) & Manes.09G039900 (PP2A)) of developing storage roots (stages 1-5). Relative expression was calculated using the $2^{-\Delta\Delta Ct}$ method in relation to stage one. X- and Y-axis of the plots show developmental stage and relative expression, respectively. Gene names are given in the plot titles. The heatmap on the top right shows the Pearson's R value of pairwise comparisons. Asterisks indicate significant correlation (FWER ≤ 0.05 as indicated by differences in asterisks). The genes were hierarchically clustered after Ward´s D2.

Figure 1

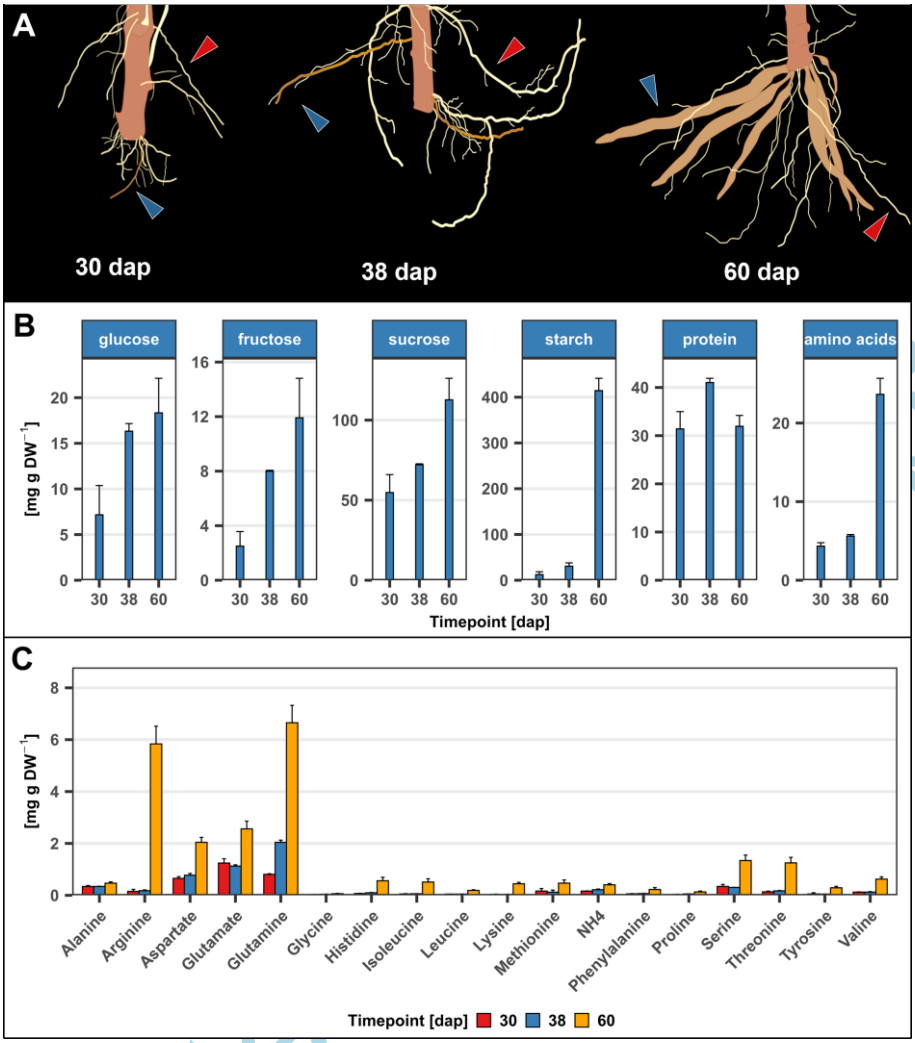

Figure 2

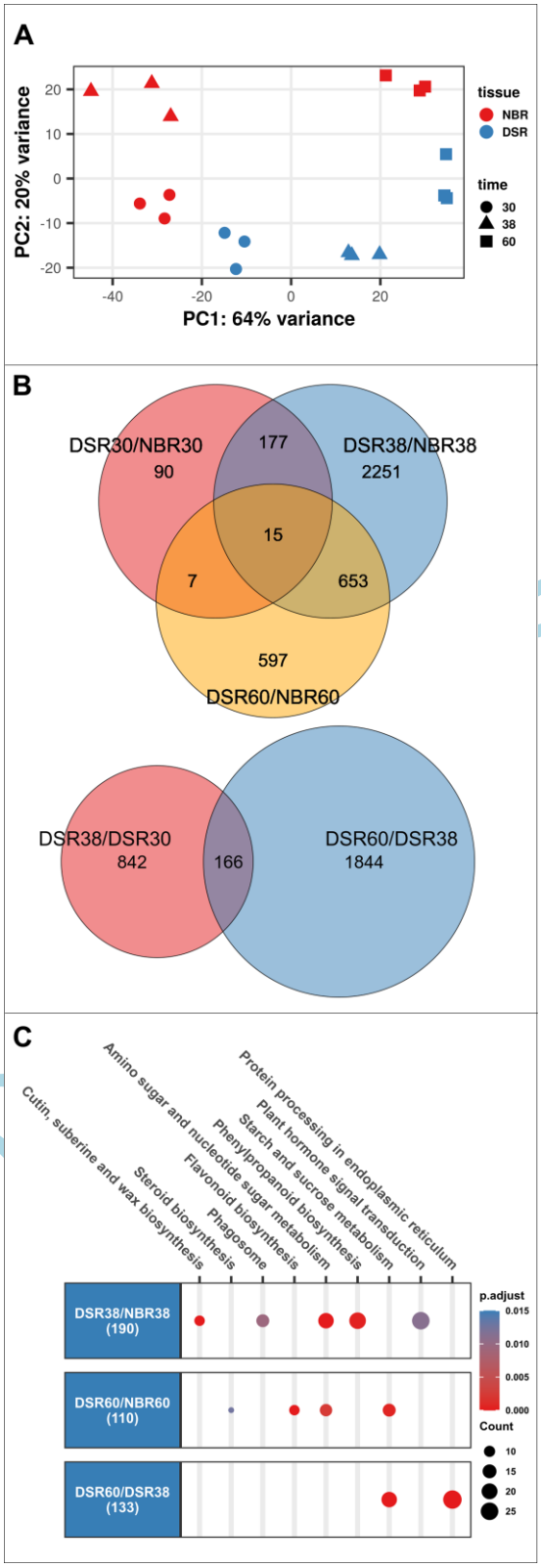

Figure 3

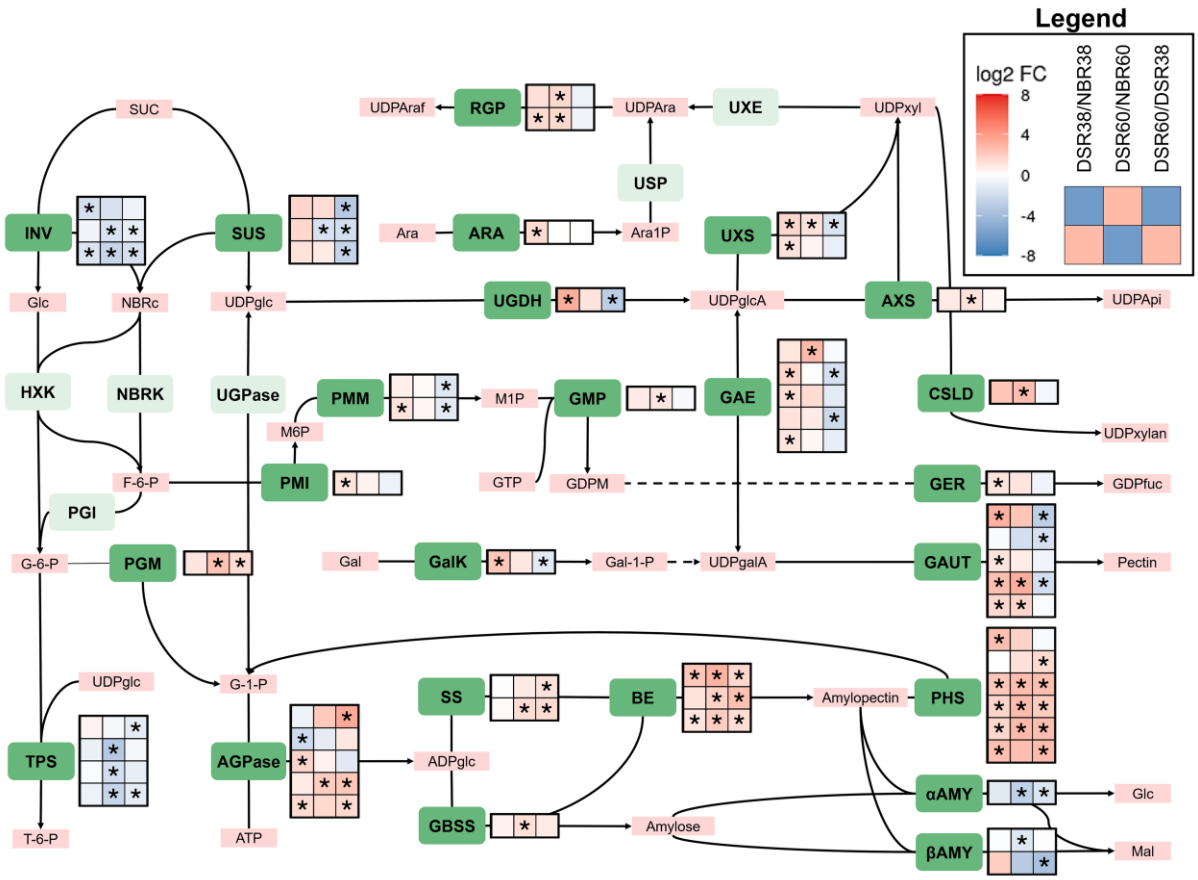

Figure 4

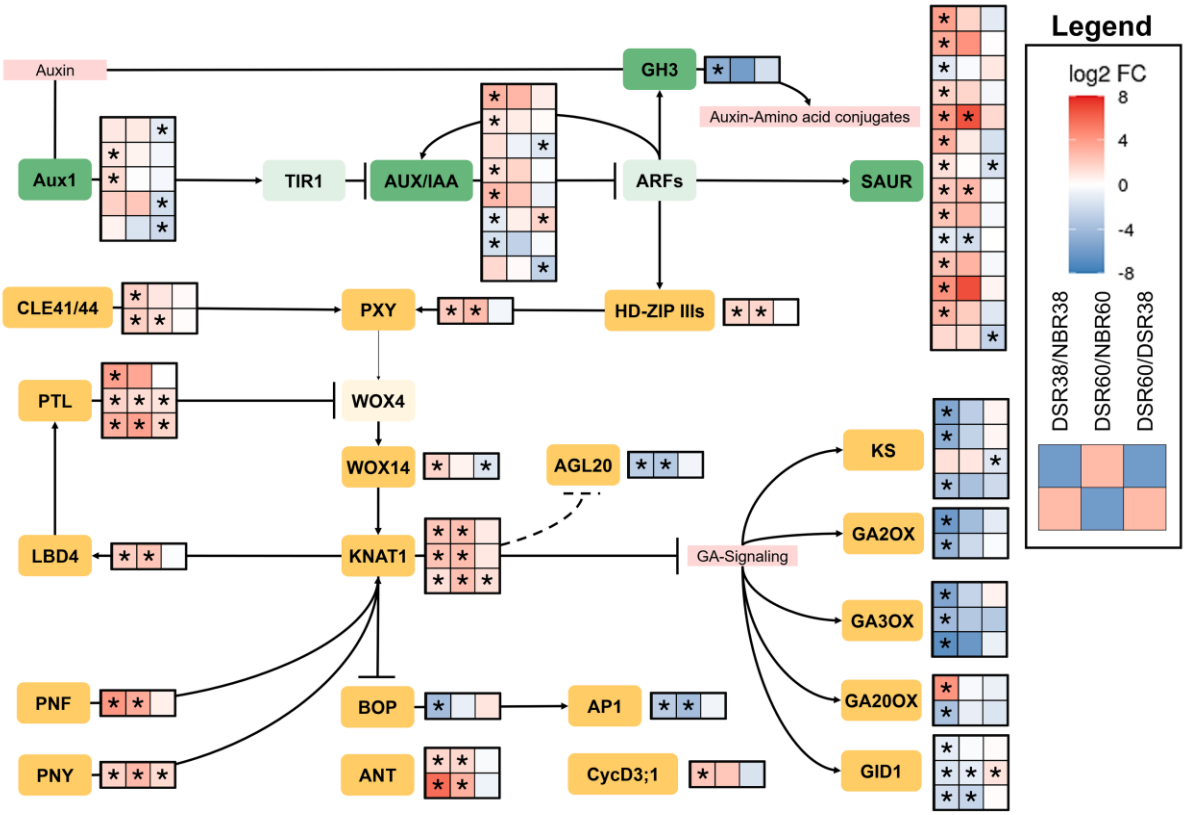

Figure 5

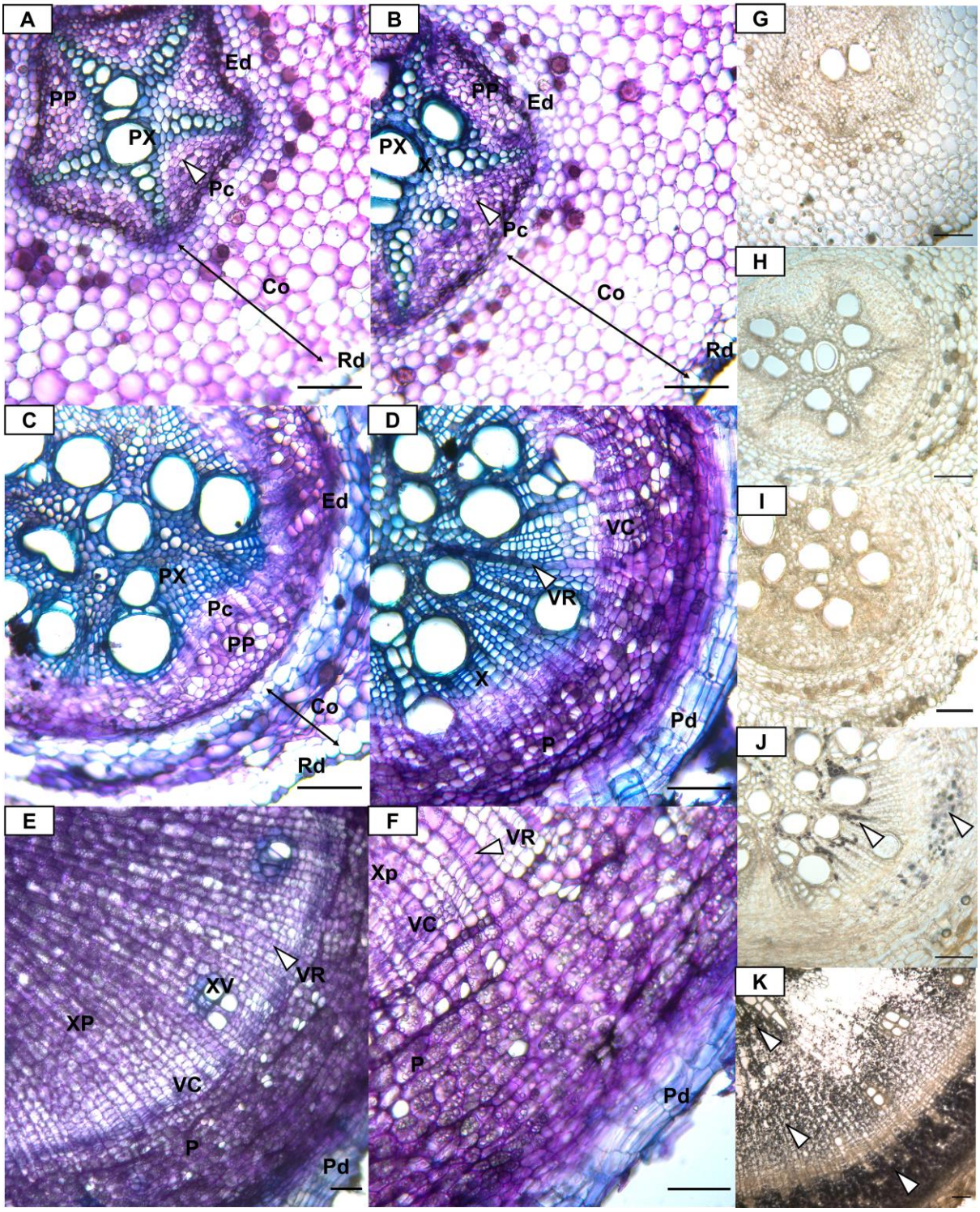

Figure 6